The speed of a wave along a fluid/solid interface in the presence of anisotropy and prestress

Andrew N. Norris

Department of Mechanical and Aerospace Engineering, Rutgers University, Piscataway, New Jersey 08855-0909

Bikash K. Sinha

Schlumberger-Doll Research, Old Quarry Road, Ridgefield, Connecticut 06877-4108

(Received 13 October 1994; accepted for publication 23 March 1995)

The classical solution for the Scholte wave along a fluid and isotropic substrate is well known. However, when the substrate is either a weakly anisotropic solid, or the adjoining fluid is subject to a hydrostatic pressure, the analysis of Scholte wave propagation becomes rather complex and lengthy computations are required to obtain the solution. The purpose of this paper is to apply simple and computationally efficient expressions in the determination of Scholte wave speeds for substrates with either weak anisotropy or in the presence of uniform initial stresses and strains in the substrate and fluid media. Both of these two simple expressions are for the incremental change in the Scholte wave speed $\Delta v/v$ from an appropriately selected isotropic, reference substrate and adjoining fluid under no hydrostatic pressure. The predictions of the Scholte wave speeds from the derived expressions agree to well within 1%-2% with the other approximation techniques for the high-frequency asymptotes of the Stoneley wave velocity dispersions in a fluid-filled borehole traversing either a weakly anisotropic formation or a formation with initial stresses and strains caused by a borehole pressurization. © 1995 Acoustical Society of America.

PACS numbers: 43.25.Fe, 43.20.Bi

INTRODUCTION

The speed of a wave along the flat interface of a twophase system comprising a uniform solid and an inviscid fluid is a function of both the anisotropy of the solid and the state of deformation and prestress in the solid and liquid. Both effects are considered here as small departures from the standard configuration of a fluid overlying an isotropic solid. Our motivation comes from the fact that acoustic measurements on rock are normally made in a fluid-filled borehole environment. Depending upon the prevailing geological stratigraphy the material symmetry axes may be obliquely oriented relative to the borehole axis, as occurs in dipping beds. As a consequence the resulting anisotropy can be rather complex in the borehole coordinates. A fast and simple means to determine the Scholte wave speed under arbitrary conditions of anisotropy is required.

Our interest in prestress and its influence on the Scholte wave is based upon the fact that the nonlinear properties of sandstone can be orders of magnitude greater than typically seen in metallic materials, ¹ as supported by data from recent experiments. ² The large nonlinearity is reflected in the magnitude of the third-order moduli relative to the second-order moduli. For example, the standard measure of fluid nonlinearity is the parameter B/A, which is approximately 5 for water. The corresponding ratio of, for example, the solid elastic moduli C_{166}/μ can be on the order of 1000 in magnitude, as it is for material II in Table II. Such enormous nonlinearity suggests that wave speeds should be very sensitive functions of confining pressure and stress. Conversely, measurement of the sensitivity of the speeds to the level of

pressure could provide a technique of determining the rock nonlinearity, in the same way that variations in the speed of Rayleigh waves as a function of the prestress applied to a solid are used to measure acoustoelastic parameters.³

The theoretical analysis of two joined fluid/solid half-spaces in a state of uniform prestress is similar in many respects to the Rayleigh wave problem for a solid only, first considered by Hayes and Rivlin⁴ and recently revisited in Ref. 5, but it is complicated by the possibility of slip at the interface between the solid and fluid. Thus the prestress can alter the material contact of particles at the fluid/solid boundary, thereby destroying the connectivity of the points in the original, or Lagrangian, description. This is a rather subtle but nontrivial difficulty, and requires a reconsideration of the basic theory of acoustoelasticity to account for this possibility. The correct formulation was described in some detail in a recent paper by Norris *et ai.*,⁶ and will be reviewed briefly below.

We consider the generic problem of this type here: the Scholte wave and its dependence upon prestress, both in the fluid and solid. The Scholte wave solution for the unstressed system is introduced in Sec. I. The effect of weak anisotropy is considered first in Sec. II. The theory of acoustoelasticity for fluid/solid composite systems is summarized and applied to the problem at hand in Sec. III. We follow the method developed by Norris *et al.*, ⁶ and use a modified stress tensor which both simplifies the traction conditions and makes the fluid stress symmetric. The results of Secs. II and III are applied in Sec. IV to two problems of relevance in borehole acoustics.

I. INTERFACE WAVES

An inviscid fluid occupies the half-space $V_f\colon x_2>0$, and solid lines in $V_s\colon x_2<0$. The wave travels in the x_1 direction, with exponential decay into the solid and no dependence upon the third direction. The dependence in the fluid is also exponential, but not necessarily decaying. A true interface wave decays in both media, whereas a "leaky" interface wave can have exponential growth in the fluid. This distinction and its consequences are discussed at greater length below. The materials are specified by the fluid density and bulk modulus ρ_f and A, respectively, by the solid density ρ_s , and the Lamé moduli λ and μ . Time harmonic motion of frequency ω is assumed.

The equations of motion in the solid and fluid are, respectively,

$$\tau_{ii,i} + \rho_s \omega^2 u_i = 0, \quad x_2 < 0,$$
 (1a)

$$A\nabla^2\phi + \rho_t\omega^2\phi = 0, \quad x_2 > 0, \tag{1b}$$

where **u** denotes the infinitesimal displacement, ϕ is the acoustic velocity potential with associated velocity $\dot{\mathbf{u}} \equiv \partial \mathbf{u}/\partial t = \nabla \phi$, and τ_{ii} are stresses in the solid:

$$\tau_{ii} = C_{iikl} u_{l,k} \,. \tag{2}$$

The notation $f_{,j} \equiv \partial f/\partial x_j$ is understood here, and the summation convention is assumed for repeated lower case Latin subscripts. The undeformed solid is isotropic with elastic moduli $C_{ijkl} = \lambda \, \delta_{ij} \, \delta_{kl} + \mu (\, \delta_{ik} \, \delta_{jl} + \, \delta_{il} \, \delta_{jk})$. The displacements for the interface wave are confined to the x_1 - x_2 plane, with $\mathbf{u} = (u_1, u_2)$, where

$$\mathbf{u} = D \operatorname{Re} \frac{i}{\omega} e^{i\omega(sx_1 - t)} \times \begin{cases} [(s, -i\alpha)e^{\omega\alpha x_2} + (\beta, -is)\operatorname{Re}^{\omega\beta x_2}], & x_2 < 0, \\ (s, i\gamma)Pe^{-\omega\gamma x_2}, & x_2 > 0, \end{cases}$$
(3)

and D has the dimensions of the square of a velocity. The phase speed along the interface is defined by the real part of the slowness s:

$$v \equiv 1/\text{Re}(s). \tag{4}$$

The Scholte wave corresponds to a real-valued s which is slower than all the other waves in the problem. However, we maintain the possibility of s being complex valued in order to consider pseudo-Rayleigh waves. The decay parameters are

$$\alpha = \sqrt{s^2 - 1/v_p^2}, \quad \beta = \sqrt{s^2 - 1/v_s^2}, \quad \gamma = \sqrt{s^2 - 1/v_f^2},$$
(5)

where $v_p = \sqrt{(\lambda + 2\mu)/\rho_s}$, $v_s = \sqrt{\mu/\rho_s}$, and $v_f = \sqrt{A/\rho_f}$ are the bulk compressional, shear, and acoustic wave speeds, respectively. The square-root function in Eq. (5) is defined such that α and β have non-negative real parts, while γ is real and positive if s is real and greater than $1/v_f$.

The complex numbers s, R, and P are found by satisfying the interface conditions, continuity of normal displacement and normal stress, and zero shear stress, which imply

$$\begin{bmatrix} \gamma & \alpha & s \\ 0 & 2s\alpha & s^2 + \beta^2 \\ \rho_f/\mu & s^2 + \beta^2 & 2s\beta \end{bmatrix} \begin{Bmatrix} P \\ 1 \\ R \end{Bmatrix} = 0.$$
 (6)

The slowness therefore satisfies the equality

$$(s^{2} + \beta^{2})^{2} - 4\alpha\beta s^{2} + \frac{\rho_{f}\alpha}{v_{s}^{4}\rho_{s}\gamma} = 0,$$
 (7)

or alternatively $F \equiv 1$, where

$$F(s,\lambda,\mu,\rho_s,A,\rho_f) = 4v_s^4 s^2 \beta(\alpha-\beta) - \frac{\rho_f \alpha}{\rho_s \gamma}.$$
 (8)

The associated wave speed is denoted as $v(\lambda, \mu, \rho_s, A, \rho_f)$. We will need the following velocities and displacement gradients in the solid for later use:

$$\dot{u}_1 = D \operatorname{Re} \{ (se^{\omega \alpha x_2} + R\beta e^{\omega \beta x_2})e^{i\psi} \}, \tag{9a}$$

$$\dot{u}_2 = D \operatorname{Im} \{ (\alpha e^{\omega \alpha x_2} + Rs e^{\omega \beta x_2}) e^{i\psi} \}, \tag{9b}$$

$$u_{1,1} = D \operatorname{Re} \{ -(s^2 e^{\omega \alpha x_2} + Rs \beta e^{\omega \beta x_2}) e^{i\psi} \}, \tag{9c}$$

$$u_{2,2} = D \operatorname{Re} \{ (\alpha^2 e^{\omega \alpha x_2} + Rs \beta e^{\omega \beta x_2}) e^{i \psi} \}, \tag{9d}$$

$$u_{2,1} = D \operatorname{Im} \{ -(s\alpha e^{\omega \alpha x_2} + Rs^2 e^{\omega \beta x_2}) e^{i\psi} \},$$
 (9e)

where $\psi = \omega(sx_1 - t)$, and R follows from Eq. (6) as $R = -2s\alpha/(s^2 + \beta^2)$.

II. WEAK ANISOTROPY

A. Isotropic reference moduli

The solid is assumed to be weakly anisotropic so that it may be approximated by an isotropic medium to leading order. We are interested in the first-order deviations of the interface wave speed from the isotropic value. Only the true interface wave, the Scholte wave, will be considered, although the later analysis for the effects of prestress is not limited in this manner. In general, the fourth-order tensor of elastic moduli display the symmetries

$$C_{iikl} = C_{iikl}, \quad C_{iikl} = C_{klii}, \tag{10}$$

reflecting the symmetry of the stress and the existence of a potential energy, respectively. There may be as many as 21 independent moduli, or $C_{IJ} = C_{JI}$ in the Voigt notation, where I = 1,2,3,4,5,6 correspond to ij = 11,22,33,23,31,12, respectively. Let

$$\hat{\lambda} = C_{12}, \quad \hat{\mu} = C_{66},$$
 (11)

and define the effective isotropic moduli associated with these Lamé constants.

$$\hat{C}_{ijkl} = \hat{\lambda} \, \delta_{ij} \, \delta_{kl} + \hat{\mu} (\, \delta_{ik} \, \delta_{jl} + \, \delta_{il} \, \delta_{jk}). \tag{12}$$

The wave speed in the anisotropic system is

$$v_{\text{anis}} = v(\hat{\lambda}, \hat{\mu}, \rho_s, A, \rho_f) + \Delta \hat{v}, \tag{13}$$

where $\Delta \hat{v}$ is the additional shift in speed due to the anisotropic elastic moduli $\hat{C}_{iikl} + \Delta C_{iikl}$, with

$$\Delta C_{ijkl} = C_{ijkl} - \hat{C}_{ijkl} \,. \tag{14}$$

It is assumed that the moduli ΔC_{IJ} are small relative to the reference isotropic ones. Standard perturbation theory can now be used.

B. The perturbation integral

The perturbation in velocity associated with the incremental moduli ΔC_{ijkl} is 7

$$\frac{\Delta \hat{v}}{v} = \frac{\int_{V_s} \Delta C_{ijkl} u_{j,i} u_{l,k} \ dV}{2 \int_{V} \rho \dot{\mathbf{u}} \cdot \dot{\mathbf{u}} \ dV}.$$
 (15)

The integral in the numerator involves the strains $u_{1,1}$, $u_{1,2}$, $u_{2,1}$, and $u_{2,2}$ through the elements of ΔC_{ijkl} with i,j,k, and l=1 and 2 only. Only four of these are nonzero: ΔC_{11} , ΔC_{22} , ΔC_{16} , and ΔC_{26} . Furthermore, the integrals involving the latter two are zero because of the fact that the strains $u_{1,1}$ and $u_{2,2}$ are exactly 90° out of phase with the strains $u_{1,2}$ and $u_{2,1}$ for the Scholte wave solution. The integrals over one wavelength in the x_1 direction therefore vanish, leaving only two independent integrals,

$$\int_{V_s} \Delta C_{ijkl} u_{j,i} u_{l,k} \ dV = \Delta C_{11} \int_{V_s} (u_{1,1})^2 \ dV + \Delta C_{22} \int_{V} (u_{2,2})^2 \ dV.$$
 (16)

The wave speed in the presence of the weak anisotropy is therefore, from Eqs. (13), (15), and (16),

$$v_{\text{anis}} = v(\hat{\lambda}, \hat{\mu}, \rho_s, A, \rho_f) + \left[\frac{(C_{11} - C_{22})}{C_{66}} \frac{I_1}{I_0} + \frac{(C_{11} + C_{22} - 2C_{12} - 4C_{66})}{C_{66}} \frac{I_2}{I_0} \right] \frac{\Gamma}{4} v,$$
 (17)

where I_0 , I_1 , I_2 , and, for later use, I_3 are defined as

$$I_0 = v_s^{-2} \int_{V_c} \dot{\mathbf{u}} \cdot \dot{\mathbf{u}} \ dV, \tag{18a}$$

$$I_1 = \int_{V_5} [(u_{1,1})^2 - (u_{2,2})^2] dV, \qquad (18b)$$

$$I_2 = \int_{V_*} [(u_{1,1})^2 + (u_{2,2})^2] dV, \tag{18c}$$

$$I_3 = \int_{V_2} [(u_{1,1})^2 + (u_{2,1})^2] dV, \tag{18d}$$

and

$$\Gamma = \left(\int_{V_{\varsigma}} \rho \dot{\mathbf{u}} \cdot \dot{\mathbf{u}} \ dV \right) \left(\int_{V} \rho \dot{\mathbf{u}} \cdot \dot{\mathbf{u}} \ dV \right)^{-1}. \tag{19}$$

The unperturbed interface waves are assumed to be wave solutions with planar phase fronts. The integrals for I_0 , I_1 , I_2 , and I_3 can then be performed over a plane of constant phase, which we select as the plane $x_1 = 0$. Furthermore, the unperturbed wave motion is independent of x_3 , and so the integral reduces to one over x_2 . The range is $0 \le x_2 < \infty$ for V_1 and $-\infty < x_2 \le 0$ for V_3 . The integrals in Eq. (18) can be

performed directly using the expressions for the velocities and displacement gradients in Eq. (9), yielding

$$I_{\rm C} = \frac{1}{v_{\rm s}^2} \left[\frac{s^2 + \alpha^2}{2\alpha} + \frac{R^2}{2\beta} (s^2 + \beta^2) + 2sR \right],\tag{20a}$$

$$I_1 = \frac{1}{v_n^2} \left[\frac{s^2 + \alpha^2}{2\alpha} + \frac{2s\beta R}{\alpha + \beta} \right],\tag{20b}$$

$$I_{2} = \frac{s^{4} + \alpha^{4}}{2\alpha} + \frac{2s\beta R}{\alpha + \beta} \left(s^{2} + \alpha^{2} \right) + s^{2}\beta R^{2}, \tag{20c}$$

$$I_3 = v_s^2 s^2 I_0. (20d)$$

Note that the four integrals are dimensionally equivalent, and they appear in Eq. (17) only as ratios of one another. We have taken advantage of these properties and removed extraneous common factors in Eqs. (20). Also, it is shown in the Appendix that

$$\Gamma = 1 - \alpha^{2} \left(1 + \frac{\gamma^{2}}{s^{2}} \right) \left\{ \frac{1}{v_{f}^{2}} - \frac{1}{v_{p}^{2}} + 4v_{s}^{4} (\alpha - \beta) [2\alpha\beta^{2} + s^{2}(\alpha - \beta)] \frac{\rho_{s}\gamma^{3}}{\rho_{f}\beta} \right\}^{-1}.$$
(21)

Also, $\Gamma \le 1$ with equality when $\rho_f = 0$, which is the Rayleigh wave limit. In summary, Eq. (17) provides a concise and simple formula to determine the Scholte wave speed for arbitrary anisotropy in the solid.

III. SMALL-ON-LARGE THEORY

A. The equations of motion

The basic system of fluid and isotropic solid is now assumed to be deformed in such a manner that the prestress and strain are compatible with the equations of static equilibrium. We are interested in the subsequent "small-onlarge" motion. In order to calculate the change in the Scholte wave speed relative to the unstressed case, one might follow the standard procedure for acoustoelastic problems, and treat the dynamics in terms of the original or Lagrangian coordinates. This approach is not suitable when both solid and inviscid fluid are present, as the following example may illustrate. A solid cube is immersed in a fluid, which is then brought to a pressure p. Scholte waves are subsequently propagated along one side of the block. An initial area of dSon the solid surface is converted into an area of (1-p)(2K)dS, where K is the solid bulk modulus. Assuming that the fluid dilates in an isotropic manner, the corresponding area of the original fluid at the interface becomes (1-p)(2A))dS. The areas are not the same, indicating the slip of fluid particles at the interface. Any description of the dynamics in terms of Lagrangian coordinates is therefore highly suspect, because of the obvious difficulty of satisfying the continuity of the Cauchy traction between the solid and fluid. In other words, the Lagrangian description is quite unsuitable for this problem. An appropriate strategy is to formulate everything in terms of the Piola-Kirchhoff stress in the "intermediate" configuration. However, it turns out that the jump in the area mapping still enters into the correct formulation of the small-on-large traction continuity conditions, thereby

making the formulation rather difficult. Furthermore, the Piola-Kirchhoff stress tensor in intermediate coordinates is not symmetric, even for an ideal fluid.

A general method for dealing with acoustoelastic problems for fluid/solid composite media is described by Norris $et\ al.^6$ The equations of motion for the small-on-large motion $\mathbf{u}(\mathbf{x},t)$ are cast in terms of the intermediate or "laboratory" coordinates \mathbf{x} , not the original coordinates. It is assumed that the liquid and solid are both subject to uniform deformation, so that the prestress in the fluid is a hydrostatic pressure p above ambient. The prestrain in the solid is defined by the initial displacement \mathbf{w} , or more to the point, by its deformation gradient with components $w_{i,j} = \partial w_i / \partial x_j$. The associated strain is $e_{ij} = (w_{i,j} + w_{j,i})/2$, with trace $e = e_{kk}$. The prestress in the solid is σ_{ij} ,

$$\sigma_{ij} = C_{ijkl} e_{kl}, \qquad (22)$$

where C_{ijkl} are the isotropic elastic moduli, with Lamé constants λ and μ . The continuity of the normal stress across the interface implies

$$\sigma_{22} = -p. \tag{23}$$

We may think of e, e_{11} , and p as the three parameters defining the prestress, in terms of which

$$e_{22} = -\frac{\lambda}{2\mu} e - \frac{p}{2\mu}, \quad e_{33} = \left(1 + \frac{\lambda}{2\mu}\right) e - e_{11} + \frac{p}{2\mu}.$$
 (24)

The difficulty of the area changes and the associated satisfaction of the traction continuity conditions is dealt with by adding a divergence-free stress, and is discussed in detail elsewhere. The small-on-large versions of Eqs. (1) and (2) become 6

$$\tilde{\tau}_{ii,i} + \tilde{\rho}_s \omega^2 u_i = 0, \quad x_2 < 0, \tag{25a}$$

$$\tilde{A}\nabla^2\phi + \tilde{\rho}_f\omega^2\phi = 0, \quad x_2 > 0, \tag{25b}$$

$$\tilde{\tau}_{ii} = \tilde{C}_{iikl} u_{l,k} \,. \tag{25c}$$

The new densities and elastic moduli are

$$\tilde{\rho}_f = \left(1 + \frac{p}{A}\right) \rho_f, \tag{26a}$$

$$\tilde{A} = \left[1 + \left(1 + \frac{B}{A} \right) \frac{p}{A} \right] A, \tag{26b}$$

$$\tilde{\rho}_s = (1 - e)\rho_s \,, \tag{26c}$$

$$\begin{split} \tilde{C}_{ijkl} &= C_{ijkl} + (\delta_{ij}\delta_{kl} - \delta_{il}\delta_{jk})p + \sigma_{ik}\delta_{jl} - C_{ijkl}w_{m,m} \\ &+ C_{ijklmn}w_{m,n} + C_{pjkl}w_{i,p} + C_{ipkl}w_{j,p} \\ &+ C_{ijpl}w_{k,p} + C_{ijkp}w_{l,p} \,, \end{split} \tag{26d}$$

where $B = \rho_f^2 d^2 p/d\rho^2|_{\rho_f}$ is the usual nonlinear modulus of a fluid, and C_{ijklmn} are the third-order moduli of the solid. Some aspects are fairly obvious, such as the dependence of the fluid density and bulk modulus on the background pressure. Similarly, the transformation $\rho_s \rightarrow \tilde{\rho}_s$ is an immediate consequence of the volumetric change under the prestrain. The stress tensor $\tilde{\tau}_{ij}$ is related to but not exactly the same as

the Piola-Kirchhoff stress in the intermediate configuration. It includes a divergence-free part proportional to the pressure p. Note that there is no mention made of the deformation in the fluid because it is arbitrary in the sense that an inviscid fluid can undergo any amount of shear deformation at no cost in energy. This is consistent with the notion that the state of an ideal fluid is defined completely by its pressure level. The derivation of these constitutive equations is rather involved, and we refer to Norris et al.6 for full details. The effective elastic constants \tilde{C}_{iikl} defined in Eqs. (25c) and (26d) without the divergence-free part proportional to the pressure p are similar to Thurston's effective elastic constants B_{iikl} in the intermediate configuration, for wave propagation in a prestressed medium.8 However, it should be carefully noted that $\tilde{C}_{iikl} = B_{iilk}$, because of a slight difference in our notation in Eqs. (25a) and (25c) and that of Thurston's notation used in Eq. (36).8

The significant feature of the model for the present purpose is that the traction and displacement continuity conditions for the small-on-large motion are in exactly the same form as those for the original equations in the unstressed configuration. The acoustoelastic equations are therefore in their natural or divergence form, which allows us to use standard methods for dealing with partial differential equations of this type, specifically standard perturbation analysis⁷ for acoustoelastic problems. We now apply the general methods of perturbation theory to estimate the change in wave speed for the interface wave of Sec. I. We approach this in two parts, first identifying new effective isotropic moduli, and then considering the increment in speed due to the deviations from this medium.

B. The isotropic moduli

The elastic moduli of Eq. (26d) satisfy the second symmetry property of Eq. (10), but not the first. The problem is therefore essentially different from that of a weakly anisotropic medium. We proceed as before by first subtracting out an isotropic part in the moduli, so that the complexity of the shifted moduli is reduced. Thus we consider the shifted isotropic moduli \hat{C}_{ijkl} of Eq. (12) where we now choose the new Lamé moduli as

$$\hat{\lambda} = \tilde{C}_{1122}, \quad \hat{\mu} = \tilde{C}_{2121}.$$
 (27)

We assume that the third-order moduli are isotropic, and let C_{IJK} stand for C_{ijklmn} according to the standard notation. The three independent third-order moduli can be taken as C_{111} , C_{112} , and C_{123} , in terms of which the others are $C_{166} = (C_{111} - C_{112})/4$, $C_{144} = (C_{112} - C_{123})/2$, and $C_{456} = (C_{166} - C_{144})/2$. It follows from Eq. (26d) that

$$\hat{\lambda} = \lambda + (\lambda + C_{112})(e_{11} + e_{22}) + (C_{123} - \lambda)e_{33} + p, \qquad (28a)$$

$$\hat{\mu} = \mu + (\mu + C_{166})(e_{11} + e_{22}) + (C_{144} - \mu)e_{33} - p.$$
 (28b)

The speed of the interface wave in the presence of the deformation is given by

$$v_{\text{def}} = v(\hat{\lambda}, \hat{\mu}, \tilde{\rho}_s, \tilde{A}, \tilde{\rho}_f) + \Delta \hat{v}, \tag{29}$$

where the perturbation $\Delta \hat{v}$ now depends upon the eight moduli ΔC_{ijkl} with i, j, k, and l=1 and 2 only, and

$$\Delta C_{ijkl} = \tilde{C}_{ijkl} - \hat{C}_{ijkl}. \tag{30}$$

It turns out that five of these are identically zero; thus

$$\Delta C_{1122} = 0, \quad \Delta C_{2121} = 0,$$

$$\Delta C_{2211} = 0, \quad \Delta C_{1212} = 2\mu(e_{11} - e_{22}),$$

$$\Delta C_{1111} = 2(\lambda + 3\mu + C_{166})(e_{11} - e_{22}), \quad \Delta C_{212} = 0,$$

$$\Delta C_{2222} = -2(\lambda + 2\mu + C_{166})(e_{11} - e_{22}),$$

$$\Delta C_{1221} = 0.$$
(31)

The first two identities in (31) are a consequence of the choice of the "background" isotropic elastic moduli \hat{C}_{ijkl} , and the second pair follow by direct calculation. Use has also been made of the fact that the prestress in the fluid and solid are in equilibrium. Specifically, the constraint (23) has been used in obtaining the final four identities in (31) for the incremental moduli ΔC_{ijkl} . It is interesting to note that

$$\Delta C_{1111} + \Delta C_{2222} - \Delta C_{1212} = 0, (32)$$

regardless of the prestress. This relation does not hold in the weakly anisotropic problem, even though the reference moduli of Eq. (11) appear to be similar to those of Eq. (27).

C. The perturbation integral

We again use the perturbation integral of Eq. (15), which applies equally well to the present acoustoelastic problem.⁶ When combined with Eqs. (31) the integrand can be considerably simplified, with the result

$$\int_{V_s} \Delta C_{ijkl} u_{j,i} u_{l,k} \, dV$$

$$= 2(e_{11} - e_{22}) \int_{V_s} dV \{ \mu [(u_{2,1})^2 + (u_{1,1})^2] + (\lambda + 2\mu + C_{166}) [(u_{1,1})^2 - (u_{2,2})^2] \}. \tag{33}$$

We have also made the replacements $(\hat{\lambda}, \hat{\mu}) \rightarrow (\lambda, \mu)$ in Eq. (33), consistent with the first-order nature of the approximation.

The leading-order correction to the phase speed after deformation now follows from Eqs. (15), (29), and (33) as

$$v_{\text{def}} = v(\hat{\lambda}, \hat{\mu}, \tilde{\rho}_s, \tilde{A}, \tilde{\rho}_f) + \left[\left(\frac{v_p^2}{v_s^2} + \frac{C_{166}}{\mu} \right) \frac{I_1}{I_0} + \frac{I_3}{I_0} \right] \times (e_{11} - e_{22}) \Gamma v, \tag{34}$$

where I_0 , I_1 , and I_3 are defined in Eq. (18), and Γ in Eq. (19). Explicit expressions are given in Appendix A for these integrals. All the formulas there are valid for either the pure subsonic interface wave (Scholte wave), or a leaky wave, as defined in the Appendix. For the Scholte wave we recover the simpler expressions of Eq. (20) for I_0 , I_1 , and I_3 , and (21) for Γ . In summary, Eq. (34) provides a relatively simple means to compute the dependence of the phase speed of Scholte interface waves on the prestress.

IV. APPLICATIONS AND EXAMPLES

We focus on two examples of relevance to borehole acoustics. We consider how anisotropy influences the flex-

TABLE I. Material properties for Bakken shale.

ρ	C11	C _{1.2}	C ₁₃	C ₃₃ (GPa)	C ₄₄
(kg/m³)	(GPa)	(GP ₁)	(GPa)		(GPa)
2230	40.9	10.3	8.5	26.9	10.5

ural or n=1 nonaxisymmetric mode in a circular fluid-filled borehole, and the pressure dependence of the speed of the axisymmetric Stoneley mode (n=0). The dispersive properties of both modes are we.l understood for undeformed isotropic configurations. They differ in their low-frequency form; the flexural wave speed becomes the speeds of shear waves in the formation, while the quasistatic limit of the Stoneley mode is known as the tube wave. Previous studies have considered the influence of weak anisotropy and borehole pressurization on the tube wave speed. The full frequency dependence of the mode under the influence of anisotropy or pressurization is discussed by Sinha et al. [11,12] We will only consider the high-frequency limits, where both modes travel with the speed of the Scholte wave for the fluid and solid.

A. High-frequency flexural waves in anisotropic formations

The high-frequency limit of the flexural or n=1 mode of a circular borehole depends only upon the conditions in the vicinity of the borehole wall. That is, the curvature of the bore wall can be neglected and all that is required to estimate the speed of the wave are the local elastic properties of the wall. Hence we can use the analysis of Sec. II to determine the flexural wave speed for arbitrary weak anisotropy.

At the same time, the wave is characterized by a sagittal plane in which the dominant motion occurs, and we need to define our coordinates to reflect the choice of plane. The deformation associated with Scholte waves in isotropic substrates with an overlying fluid is exclusively in the sagittal plane containing the surface normal and propagation direction. On the other hand, deformation associated with such waves in arbitrarily anisotropic substrates may have deformation components both parallel and normal to the sagittal plane. This type of deformation occurs because of the coupling between the SH- and SV-wave polarizations. However, for materials with transversely isotropic (TI) symmetry, the SH waves are always decoupled from the qSV waves for any propagation direction. Consequently, it is expedient to consider Scholte wave propagation along a given direction with deformation in either of the two orthogonal sagittal planes. The two sagittal planes contain the propagation direction and either the SH- or qSV-wave polarization.

As an illustrative example, consider Bakken shale as a TI substrate material with x_3 as the TI-symmetry axis. The anisotropic constants of this material are shown in Table I. Calculations have been performed from Eq. (17) for the Scholte wave speed for motion in the sagittal plane containing the propagation direction and surface normal along x_1 and x_2 directions, respectively. The deformation associated with the Scholte waves corresponds to the qSV-wave polarization. The other orthogonal Scholte wave solution for

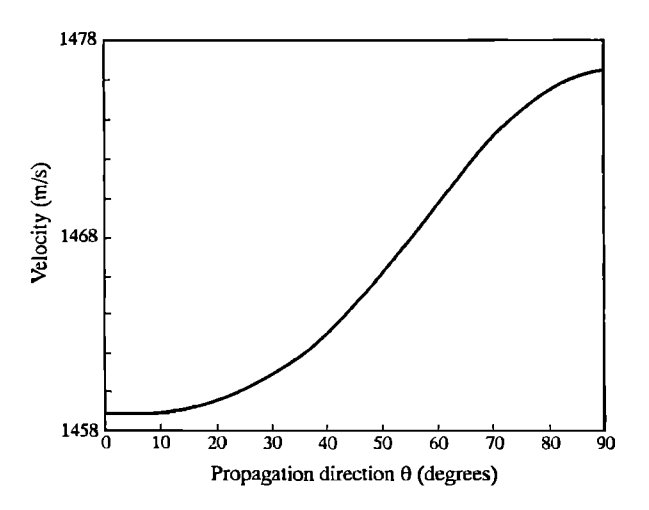


FIG. 1. Scholte wave velocity as a function of propagation direction θ from the TI-symmetry axis. Results are for deformation in the qSV-polarization plane in Bakken shale.

propagation along the same x_1 direction corresponds to the SH-wave polarization. The propagation direction is being measured from the TI-symmetry axis. The anisotropic elastic constants required for a propagation direction θ measured from the TI-symmetry axis are readily obtained by an orthogonal transformation of elastic constants referred to the principal axes. The angle θ denotes a rotation about the x_2 axis. The transformation relationship for the elastic constants in the compressed Voigt's notation is explicitly given in Refs. 11 and 13.

Figure 1 shows the Scholte wave speed as a function of the propagation direction θ as calculated from Eq. (17). The Scholte wave speeds are for deformation in the sagittal plane containing the qSV polarization. The isotropic constants for the unperturbed solution are given by Eq. (11). Comparison of the Scholte wave speeds for the four propagation directions (θ =0°, 45°, 60°, and 90°) with the high-frequency asymptotes of the qSV-polarized flexural waves in Fig. 4(b) of Ref. 11 shows the correct trend for the high-frequency limit of the flexural wave speeds. The differences between the Scholte wave and flexural wave speeds at 10 kHz are approximately on the order of 3%. However, a part of these differences is due to the fact that the flexural wave dispersions have not yet "saturated" at 10 kHz. It should also be noted that other choices for the aforementioned isotropic constants yield slightly different values for the Scholte wave speed. As is the case with any perturbation model, the background solution should be selected so that the perturbative deviation of the Scholte wave speed from the isotropic case is relatively small due to the material anisotropy.

B. High-frequency waves in a pressurized borehole

We now turn to the pressure dependence of the Stoneley wave speed in a circular borehole. The low-frequency, or tube wave, behavior under pressurized conditions has been analyzed in some detail by Johnson *et al.*¹ The full description of the pressurized Stoneley mode over the entire frequency range of interest is discussed in a separate paper.¹² Here we address the high-frequency end of the spectrum, where the 2-D analysis of Sec. III is directly applicable.

The deformation associated with the prestress is a positive hydrostatic pressure p in the fluid and a nonuniform deviatoric plane strain field in the solid. The plane of strain is perpendicular to the borehole axis, and the principal strain axes are the radial and circumferential directions, with strains $-p/2\mu$ and $p/2\mu$ at the bore wall, respectively. This is an example of a slip surface because of the different area mapping on either side of the boundary. Thus the virgin area dS on the solid surface is increased to $(1+p/(2\mu))dS$. Assuming the fluid is compressed axially as a plug of length L while it expands laterally, then the length of the plug after compression is $(1+p(A^{-1}+\mu^{-1}))L$. It follows that the area dS on the fluid side of the surface decreases to $[1+p(A^{-1}+(2\mu)^{-1})]dS$. The point is that the concept of Lagrangian coordinates is clearly of little or no utility in dealing with the interface, and one needs to resort to a theory of the type presented in Sec. III and discussed in Ref. 6.

The high-frequency limit of the modal wave speed depends upon the prestress conditions in the vicinity of the bore wall. Thus, with the Cartesian x_1 , x_2 , and x_3 , axes replacing the axial, radial, and azimuthal directions, we have

$$e_{11}=0, \quad e_{22}=-e_{33}=-p/2\mu.$$
 (35)

The deformed isotropic elastic density and moduli are therefore, from Eqs. (26) and (28),

$$\tilde{\rho}_s = \rho_s, \quad \hat{\lambda} = \lambda - (\lambda - \mu + C_{144}) \frac{p}{\mu},$$

$$\hat{\mu} = \mu - (2\mu + C_{456}) \frac{p}{\mu}.$$
(36)

The perturbed wave speed is then given by Eqs. (34)–(36). Note that the shift in v depends upon two of the three third-order elastic moduli, viz., C_{144} and $C_{166} = C_{144} + 2C_{456}$.

The properties of two distinct rock types are listed in Table II, along with the Scholte wave speed for water overlying the solid. The nonlinear parameter for water is taken as B/A = 5. Table II also gives the Scholte wave speeds for pressure levels of 2000 psi (13.8 MPa) in rock I and 500 psi (3.45 MPa) in II, as computed from Eq. (34). Rock II is

TABLE II. Material properties of the two rock materials. The parameters for rock II are for a dry Berea sandstone.

Rock	ρ (kg/m³)	λ (GPa)	μ (GPa)	υ _ρ (m/s)	υ _s (m/s)	υ (m/s)	C ₁₄₄ (GPa)	C ₁₆₆ (GPa)	p (MPa)	υ + Δυ (m/s)
1	2135	19.5	6.5	3022	1745	1332	193	-578	13.8	1381
II from Ref. 14	2062	11.1	4.64	2320	1500	1156	2702	-4543	3.45	1257

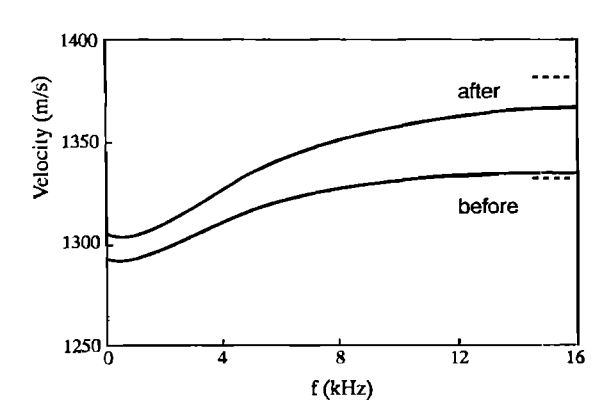


FIG. 2. Stoneley wave dispersions before and after borehole pressurization of 2000 psi. Results are for a borehole of diameter 8 in. surrounded by formation I. The dashed lines are the Scholte wave speeds from Table II.

much more nonlinear than I, hence the smaller value of pressure considered. In both cases the changes in the fluid properties are insignificant compared with those for the solid moduli. Thus, at the higher pressure of 13.8 MPa, we have $\tilde{\rho}_f/\rho_f=1.006$, $\tilde{A}/A=1.037$. In comparison, we have $\hat{\lambda}/\lambda=0.94$ and $\hat{\mu}/\mu=1.12$ for formation I at p=13.8 MPa, whereas the same quantities are $\hat{\lambda}/\lambda=2.10$ and $\hat{\mu}/\mu=1.15$ for formation II at 25% the same pressure level. The large value of $\hat{\lambda}/\lambda$ in the latter case means that the present theory is limited to low-pressure levels for rocks with such strong nonlinearity.

Figures 2 and 3 show how these nondispersive calculations compare with the numerical results of a perturbation analysis for the Stoneley wave mode in a borehole of radius 0.1016 m. The theory behind these curves is described in a separate paper. The horizontal dashed lines show the non-dispersive Scholte wave speeds before and after borehole pressurization. We note that agreement with the dispersive theory for both rocks I and II is well within 1%-2%. A part of the discrepancy for rock II can be partly ascribed to the strongly nonlinear nature of this rock. However, we believe the discrepancy is in equal measure due to the fact that the dispersion curve for the undeformed rock II has not "saturated" even at the relatively high frequencies considered. The deformed curve, on the other hand, is flat at the high-frequency end, and the discrepancy between the limiting

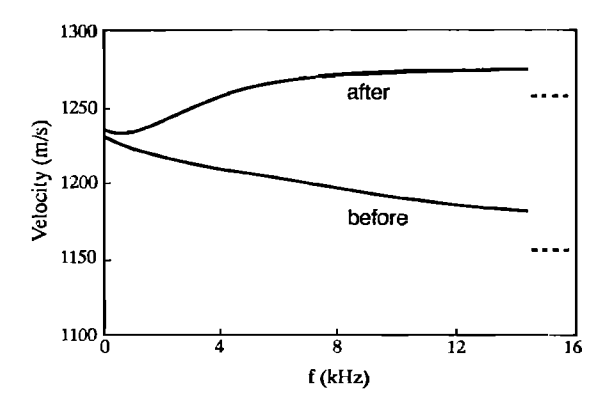


FIG. 3. Dispersion curves for the Stoneley wave with and without pressurization of 500 psi. The computation is for a borehole of diameter 8 in. surrounded by formation II, and the dashed lines are from Table II.

speed and the Scholte wave estimate is comparable to the deviation of the undeformed dispersion curve from the undeformed Scholte wave speed.

V. CONCLUSION

The speed of a Scholte wave in a slightly anisotropic medium is given by formula (17), where the effective isotropic moduli λ and $\hat{\mu}$ are defined in Eq. (11). The Scholte wave speed in a system under arbitrary initial stress is given by Eq. (34), where the reference isotropic constants are given by Eqs. (26a)-(26c) and (28). In either case, the remaining quantities I_0 , I_1 , I_2 , I_3 , and Γ follow from Eqs. (20) and (21) with the reference isotropic moduli and densities used in these expressions. The formula for the wave speed in the presence of prestress can also be applied to consider leaky pseudo-Rayleigh waves, with the necessary modification to Eq. (34) discussed in the Appendix. We stress the simplicity of the expressions for the modified wave speeds. The only computational difficulty involved is to find the roots of the standard equation for Scholte waves in the isotropic configuration. Everything else is explicit and easily computed for arbitrary conditions of anisotropy and prestress. The examples given illustrate the utility of the theory for estimating the speed of borehole waves in anisotropic and prestressed rock formations.

ACKNOWLEDGMENTS

The authors would like to thank A. K. Booer for support and valuable comments on the manuscript. Part of this work was performed while the first author was a visitor at Schlumberger-Doll Research, Ridgefield, CT.

APPENDIX: THE NUMBER Γ AND OTHER INTEGRALS

The integral in the denominator of Eq. (15) is clearly a measure of the total energy of the wave mode considered. The associated integral is over the full range $-\infty < x_2 < \infty$. If the wave motion considered is subsonic relative to all bulk wave speeds, $v < v_{\alpha}$ with $\alpha = f$, s, and p, then the wave is a true interface wave in the sense that it decays exponentially away from the interface. This is the "Scholte" wave, and its kinetic energy is bounded. We are also interested in "leaky" interface waves, specifically the "pseudo-Rayleigh" wave that occurs when the Rayleigh wave speed exceeds the fluid bulk wave speed. This is not a true interface wave in the sense of the Scholte wave. The reasons are various, but all stem from the fact that the slowness root for s lies on the "wrong" Riemann sheet for the square-root function y. The root corresponds to a value of γ which yields a solution that grows exponentially in the fluid as the field point recedes from the interface. The wave motion still decays in the solid half-space. However, the exponential growth in the fluid indicates that the kinetic energy in the denominator of Eq. (15) is not defined for such a wave mode. It is clearly meaningless to ascribe a finite energy to this wave solution, which is another indication of the unphysical nature of the pseudo-Rayleigh wave considered in isolation.

In order to include the possibility of considering leaky waves, we use an analytical device to remove the kineticenergy integral in favor of a similar integral over the solid region only, which is finite and has physical meaning. Consider the variation of s for a uniform change in the fluid density ρ_f . The shift is determined from the identity

$$\frac{\partial s}{\partial \rho_f} = -\left(\frac{\partial F}{\partial \rho_f}\right) \left(\frac{\partial F}{\partial s}\right)^{-1},\tag{A1}$$

which, combined with Eq. (4), implies

$$\frac{\Delta v}{v} = \Delta \rho_f v \operatorname{Re} \left(\frac{\partial F I \partial \rho_f}{\partial F I \partial s} \right). \tag{A2}$$

At the same time, the shift in phase speed caused by a change in the fluid density only can be determined by perturbation theory as

$$\frac{\Delta v}{v} = \frac{-\int_{V_f} \!\! \Delta \rho_f \dot{\mathbf{u}} \cdot \dot{\mathbf{u}} \; dV}{2\int_{V} \!\! \rho \dot{\mathbf{u}} \cdot \dot{\mathbf{u}} \; dV} = -\frac{\Delta \rho_f}{2\rho_f} + \frac{\Delta \rho_f}{2\rho_f} \frac{\int_{V_s} \!\! \rho \dot{\mathbf{u}} \cdot \dot{\mathbf{u}} \; dV}{\int_{V} \!\! \rho \dot{\mathbf{u}} \cdot \dot{\mathbf{u}} \; dV}. \tag{A3}$$

Comparison of Eqs. (19), (A2), and (A3) yields the identity

$$\Gamma = 1 + 2 \frac{\rho_f}{v} \frac{\partial v}{\partial \rho_f} = 1 + 2v \rho_f \operatorname{Re} \left(\frac{\partial F/\partial \rho_f}{\partial F/\partial s} \right). \tag{A4}$$

The real number Γ now follows from Eqs. (8), (19), and (A4) as

$$\Gamma = 1 - v \operatorname{Re} \left\{ \frac{\alpha^2 (s + \gamma^2 / s)}{(1/v_f^2) - (1/v_\rho^2) + 4v_s^4 (\alpha - \beta)[2\alpha \beta^2 + s^2 (\alpha - \beta)] \rho_s \gamma^3 / \rho_f \beta} \right\}.$$
(A5)

The parameters s, β , α , γ , and -R are all real positive numbers for the Scholte wave, and the phase speed is simply v = 1/s. Both numerator and denominator of the bracketed quantity in Eq. (A5) are real positive numbers, and Γ reduces to Eq. (21).

Finally, we provide expressions for the integrals I_0 , I_1 , and I_3 in Eqs. (34) when the wave is not a pure interface mode. Then s is complex valued, and we find from Eqs. (9) and (18) that

$$I_j = \frac{1}{2} \operatorname{Re}(J_j + K_j), \quad j = 0, 1, \text{ and } 3 \text{ (no sum)}, \quad (A6)$$

where J_0 , J_1 , and J_3 are given by the right-hand members of the expressions for I_0 , I_1 , and I_3 in Eq. (20), and

$$K_{0} = \frac{|s|^{2} + |\alpha|^{2}}{\alpha + \bar{\alpha}} + |R|^{2} \left(\frac{|s|^{2} + |\beta|^{2}}{\beta + \bar{\beta}}\right) + 2R \left(\frac{s\bar{\alpha} + \bar{s}\beta}{\bar{\alpha} + \beta}\right),$$

$$K_{1} = |s|^{2} K_{0}, \quad K_{2} = \frac{|s|^{4} - |\alpha|^{4}}{\bar{\alpha} + \bar{\alpha}} + \frac{2s\beta R}{(\bar{\alpha} + \beta)v_{p}^{2}},$$
(A7)

with the bar over a quantity indicating the complex conjugate.

¹D. L. Johnson, S. Kostek, and A. N. Norris, "Nonlinear tube waves," J. Acoust. Soc. Am. 96, 1829–1843 (1994).

²G. D. Meegan, P. A. Johnson, R. A. Guyer, and K. R. McCall, "Observation of nonlinear behavior in sandstone," J. Acoust. Soc. Am. 94, 3387–3391 (1993).

³ Y. H. Pao, W. Sachse, and H. Fukuoka, "Acoustoelasticity and ultrasonic measurements of residual stress," in *Physical Acoustics*, edited by W. P. Mason and R. N. Thurston (Academic, New York, 1984), Vol. 17, pp. 62–143.

⁴M. Hayes and R. S. Rivlin, "Surface waves in deformed elastic materials," Arch. Rat. Mech. Anal. 8, 358-380 (1961).

⁵A. N. Norris (unpublished).

⁶ A. N. Norris, B. K. Sinha, and S. Kostek, "Acoustoelasticity of solid/fluid composite systems," Geophys. J. Int. 118, 439-446 (1994).

⁷B. K. Sinha, "Elastic waves in crystals under a bias," Ferroelectrics **41**, 62–73 (1982).

⁸R. N. Thurston, "Effective elastic coefficients for wave propagation in crystals under stress," J. Acoust. Soc. Am. 37, 348-356 (1965); 37, 1147(E) (1965).

⁹J. E. White, *Underground Sound* (Elsevier, Amsterdam, 1983).

¹⁰ A. N. Norris and B. K. Sinha, "Weak elastic anisotropy and the tube wave," Geophysics 58, 1091-1098 (1993).

¹¹B. K. Sinha, A. N. Norris, and S. K. Chang, "Borehole flexural modes in anisotropic formations," Geophysics 59, 1037-1052 (1994).

¹²B. K. Sinha, S. Kostek, and A. N. Norris (unpublished).

¹³B. A. Auld, Acoustic Fields and Waves in Solids (Wiley, New York, 1973), Vols. I and II.

¹⁴K. W. Winkler (private communication).